

# What happens to diffusion model likelihood when your model is conditional?

Mattias Cross  
and Anton Ragni

MCROSS2@SHEFFIELD.AC.UK

A.RAGNI@SHEFFIELD.AC.UK

*Speech and Hearing (SPandH), Dept. of Computer Science, The University of Sheffield, UK*

**Editors:** C. Coelho, B. Zimmering, M. Fernanda P. Costa, L.L. Ferrás, O. Niggemann

## Abstract

Diffusion Models (DMs) iteratively denoise random samples to produce high-quality data. The iterative sampling process is derived from Stochastic Differential Equations (SDEs), allowing a speed-quality trade-off chosen at inference. Another advantage of sampling with differential equations is *exact* likelihood computation. These likelihoods have been used to rank unconditional DMs and for out-of-domain classification. Despite the many existing and possible uses of DM likelihoods, the distinct properties captured are unknown, especially in conditional contexts such as Text-To-Image (TTI) or Text-To-Speech synthesis (TTS). Surprisingly, we find that TTS DM likelihoods are agnostic to the text input. TTI likelihood is more expressive but cannot discern confounding prompts. Our results show that applying DMs to conditional tasks reveals inconsistencies and strengthens claims that the properties of DM likelihood are unknown. This impact sheds light on the previously unknown nature of DM likelihoods. Although conditional DMs maximise likelihood, the likelihood in question is not as sensitive to the conditioning input as one expects. This investigation provides a new point-of-view on diffusion likelihoods.

**Keywords:** Diffusion models, score-based generative modelling, likelihood

## 1. Introduction

DMs learn to estimate a data distribution that can be sampled from, specifically through estimating the noise of an iterative denoising diffusion process. This training scheme can be seen as Variational Lower Bound (VLB) maximization (Ho et al., 2020; Yang et al., 2023). A desirable feature of DMs is exact likelihood computation, where the likelihood of samples appearing in a data distribution can be calculated. Likelihood is predominantly used as an objective evaluation metric for sample quality. Although DMs are popular for text-guided synthesis, only unconditional tasks such as image-synthesis have focussed on likelihood. There is limited analysis on whether likelihood is a useful feature for conditional models, as used for TTI and TTS. Considering that DMs aim to maximize likelihood, learning what properties the likelihood has provides valuable research. This paper forms an initial survey on how likelihoods can be used in conditional scenarios and reviews any unexpected behaviour observed. We explore Stable Diffusion XL (SDXL) (Podell et al., 2023), a TTI model that uses Classifier-Free Guidance (CFG) (Ho and Salimans, 2022) to generate images that depict text-prompts, and Grad-TTS (Popov et al., 2021), a TTS model that uses a Mean-Reverting Variance-Preserving (MR-VP) SDE to synthesise speech given a transcript. An acceptable assumption is that a conditional likelihood is a function that is sensitive to the input data. We test this assumption through a series of experiments

on both models, and find that, for both conditioning mechanisms, there is a lack of insight as to how a conditional likelihood works. For example, SDXL likelihood cannot reliably pair images and captions. For Grad-TTS, we find likelihood is attributed voice quality and clean audio, but not intelligibility, leading to cases where audio sounds clean and the target speakers voice is correctly synthesised, but the speech is unintelligible.

## 2. Background

### 2.1. Diffusion models

DMs are usually viewed as denoisers. They are formulated as a Markovian process (Sohl-Dickstein et al., 2015; Ho et al., 2020), or with SDEs (Song et al., 2021b), as demonstrated in this study. A DM models a diffusion process from prior distribution  $p_T(\mathbf{X})$  to data distribution  $p_0(\mathbf{X})$ . Given a forward noising process from  $t = 0$  to  $t = T$  where  $T$  is the terminal time-step, it is possible to transform a data sample  $\mathbf{X}_0$  (e.g. an image or Mel-spectrogram) to a Gaussian sample  $\mathbf{X}_T$  through a SDE (Eq. 1) with drift  $\mathbf{F}(\cdot)$  w.r.t.  $t$  and diffusion  $g(\cdot)$  w.r.t. the Wiener process  $\mathbf{W}$ .

$$d\mathbf{X} = \mathbf{F}(\mathbf{X}, t)dt + g(t)d\mathbf{W} \quad (1)$$

Eq. 1 is expressed by the following reverse-SDE when running backwards in time (Anderson, 1982)

$$d\mathbf{X} = [\mathbf{F}(\mathbf{X}, t) - g(t)^2 \nabla_{\mathbf{X}} \log p_t(\mathbf{X})]dt + g(t)d\hat{\mathbf{W}} \quad (2)$$

The gradient of the log-density  $\nabla_{\mathbf{X}} \log p_t(\mathbf{X})$  is intractable, so it is estimated with a score-model  $\mathbf{S}_\theta(\cdot)$ , a neural network trained with score matching (Hyvärinen, 2005; Song et al., 2019; Vincent, 2011). Song et al. (2021b) find that there is a deterministic counterpart to a reverse SDE 2, named a *probability flow* Ordinary Differential Equation (ODE) (Eq. 3a)

$$d\mathbf{X} = [\mathbf{F}(\mathbf{X}, t) - \frac{1}{2}g(t)^2 \nabla_{\mathbf{X}} \log p_t(\mathbf{X})]dt \quad (3a)$$

$$\mathbf{H}_\theta(\mathbf{X}, t) = \mathbf{F}(\mathbf{X}, t) - \frac{1}{2}g(t)^2 \mathbf{S}_\theta(\mathbf{X}, t) \quad (3b)$$

For inference, a trained score-model is used (Eq. 3b). The formulation of  $\mathbf{H}_\theta(\mathbf{X}, t)$  is an example of a Neural ODE (NODE) (Chen et al., 2019). The connection with NODEs allows *exact* likelihood computation of the ODE/SDE, which is the focus of this paper (Further addressed in Section 3). Given that  $p_T(\mathbf{X}_T)$  is similar to Gaussian noise, one can sample a Gaussian distribution and predict a real-sample  $\mathbf{X}_0$  with a probability flow ODE (Eq. 3b).

### 2.2. Grad-TTS

Grad-TTS (Popov et al., 2021) is a TTS model that forms initial distributions centred on text encodings  $\mathbf{E}_\theta(\mathbf{y})$  and applies a diffusion decoder to denoise into Mel-spectrograms. Grad-TTS uses a linear noise schedule (Eq. 4) and an MR-VP SDE (Eq. 5) with ODE equivalent (Eq. 6).

$$\beta(t) = \beta_0 + (\beta_T - \beta_0)t \quad (4)$$

$$d\mathbf{X} = \frac{1}{2}(\mathbf{E}_\theta(\mathbf{y}) - \mathbf{X})\beta(t)dt + \sqrt{\beta(t)}d\mathbf{W} \quad (5)$$

$$d\mathbf{X} = \frac{1}{2}((\mathbf{E}_\theta(\mathbf{y}) - \mathbf{X}) - \mathbf{S}_\theta(\mathbf{X}, t, \mathbf{E}_\theta(\mathbf{y})))\beta(t)dt \quad (6)$$

The MR-VP SDE method used for modelling the conditional distribution  $p_0(\mathbf{X}|\mathbf{y})$  is different to CFG. Unlike CFG, there is no weighting parameter to control conditioning. We aim to clarify such differences in conditional methods. We experiment with this model as it is the first DM for Mel-spectrogram decoding.

### 2.3. Stable diffusion XL

SDXL is a latent DM for TTI that boasts the highest Parti Prompts score.<sup>1</sup> It performs efficient sampling by processing images through a pretrained encoder and applying DM training within the latent space. The score estimator is a conditional U-Net (Ronneberger et al., 2015) that takes image latent  $\mathbf{X}_t$  and OpenCLIP/CLIP text embeddings (Radford et al., 2021; Ilharco et al., 2021). In this work, we denote any network that encodes text  $\mathbf{y}$  as  $\mathbf{E}_\theta(\cdot)$ . Although SDXL was trained on multiple image sizes, sample quality is best for  $1024 \times 1024$ . SDXL uses a sub-linear noise-schedule,

$$\beta(t) = (\sqrt{\beta_0} + (\sqrt{\beta_T} - \sqrt{\beta_0})t)^2 \quad (7)$$

which is a time-dependant function that controls how much noise is added at each time-step. The cumulative perturbation of  $\beta(t)$ , known as denoising diffusion implicit sampling (Song et al., 2022), is given by

$$\sigma(t) = \sqrt{\frac{1 - \bar{\alpha}(t)}{\bar{\alpha}(t)}} \quad (8)$$

where  $\bar{\alpha}(t) = \prod_{s=0}^t \alpha(s)$  and  $\alpha(t) = 1 - \beta(t)$ . leading to the following ODE

$$d\mathbf{X} = \mathbf{S}_\theta \left( \frac{\mathbf{X}}{\sqrt{\sigma(t)^2 + 1}}, t, \mathbf{E}_\theta(\mathbf{y}) \right) d\sigma(t) \quad (9)$$

We refer readers to Song et al. (2022, 2021b) for the variance-exploding SDE that Eq. 9 is derived from. To generate images that depict text prompts, CFG (Eq. 10) (Ho and Salimans, 2022) is used to condition model outputs on the text input by mixing the conditional ( $\mathbf{E}_\theta(\mathbf{y})$ ) and unconditional ( $\mathbf{0}$ ) model outputs

$$\mathbf{S}_\theta(\mathbf{X}, t, \mathbf{E}_\theta(\mathbf{y}))^{(\omega)} = \mathbf{S}_\theta(\mathbf{X}, t, \mathbf{0}) + \omega[\mathbf{S}_\theta(\mathbf{X}, t, \mathbf{E}_\theta(\mathbf{y})) - \mathbf{S}_\theta(\mathbf{X}, t, \mathbf{0})] \quad (10)$$

This introduces a *guidance scale* parameter  $\omega$  that controls the weight of the conditional output. Although increasing guidance improves sample accuracy, it trades sample quality. It is assumed that CFG models a conditional distribution  $p_0(\mathbf{X}|\mathbf{y})$ , but the nuances of this assumption are clarified in this paper (Section 4.2). We choose this model as it is the most accessible large TTI DM at the time of writing.

---

1. At the time of writing, SDXL has a score of 33%, 11% higher than the next best model. <https://huggingface.co/spaces/OpenGenAI/parti-prompts-leaderboard>

### 3. Diffusion likelihood computation

Albeit the lack of investigation into exact DM likelihoods, they are extensively applied in numerous contexts.<sup>2</sup> Exact DM likelihood is computed with the instantaneous change-of-variables formula (Chen et al., 2019; Grathwohl et al., 2018):

$$\log p_0(\mathbf{X}_0) = \log p_T(\mathbf{X}_T) + \int_0^T \nabla \cdot \mathbf{H}_\theta(\mathbf{X}, t) dt \quad (11)$$

Where  $\mathbf{H}_\theta$  is a probability flow ODE (Eq. 3b). Computing the exact divergence  $\nabla \cdot \mathbf{H}_\theta(\mathbf{X}_t, t)$  is intractable, but can be estimated with the Skilling-Hutchinson trace estimator (Skilling, 1989; Hutchinson, 1989).

$$\nabla \cdot \mathbf{H}_\theta(\mathbf{X}, t) = \mathbb{E}_{p(\epsilon)}[\epsilon^\top \nabla \mathbf{H}_\theta(\mathbf{X}, t) \epsilon] \quad (12)$$

where  $\epsilon$  is a random variable. The divergence integral  $\int_0^T \nabla \cdot \mathbf{H}_\theta(\mathbf{X}, t) dt$  can be solved with a black-box ODE solver e.g. dopri5/RK45 (Dormand and Prince, 1980). Many ODE solvers are efficiently implemented with `torchdiffeq` Chen et al. (2019). With a trained score-model, the likelihood  $\log p_0(\mathbf{X}_0)$  is exact and can be used to measure the likelihood of a generated sample  $\mathbf{X}_0$ .

The relationship between likelihood and sample quality can be ambiguous (Theis et al., 2016). There is a trend for likelihood-based models that improve likelihood degrading other evaluation metrics e.g. Fréchet Inception Distance (FID), without degrading visual quality (Song et al., 2021a). Although important for evaluation, likelihood theory has alternatively been used for improved training and other tasks. Popov et al. and Song et al. use a likelihood-weighted upper bound to train models with better likelihood. Lu et al. estimate the likelihood to formulate high-order score matching, they stress the lack of understanding of  $\log p_0(\mathbf{X}_0)$  yet produce good samples by maximising likelihood. DM likelihoods can be applied to other tasks such as determining if a sample was used in training (membership inference (Hu and Pang, 2023)) and out-of-domain detection (Graham et al., 2023). Popov et al. evaluate Grad-TTS with likelihood, but it is left unspecified whether this likelihood is conditional to the input text or not.

The implications of using *conditional* probability flow ODEs (Eq. 10; 6) are under-explored. This paper provides empirical confirmation on the current state of conditional DM likelihoods. Conditional likelihoods should correlate to high quality samples, but also compatibility between the generated sample and the conditioning signal. Although this assumption is intuitive, we demonstrate DM likelihood does not reflect compatibility as expected.

Diffusion classifiers show that VLB performs well on conditional tasks. Image classification with DMs is alternative task that DMs have been applied to (Li et al., 2023; Clark and Jaini, 2023). Diffusion classifiers use VLB as a proxy for likelihood to speed up computation. Although they have impractical inference time, they are useful for diagnosing DMs, such as textual robustness. Nevertheless, there is no agreed definition for likelihood e.g. is it likelihood that a sample is from the training set? Is it the likelihood that a sample belongs to a given class? As there is no standard interpretation of what likelihood means, hence we explore the properties of likelihood.

2. The use of “exact” is used to distinguish from lower and upper bounds, in practice we use an estimation of the “exact” likelihood.

## 4. Experiments

### 4.1. Text-to-speech

The datasets we consider are the validation sets of LJSpeech (Ito and Johnson, 2017) and TED-LIUM (Rousseau et al., 2012). The LJSpeech split contains around 1 hour of audiobooks read from a US-English female speaker. The TED-LIUM split contains around 3 hours of male speakers and 1 hour of female speaker TED conference audio. To observe how likelihood changes during the denoising diffusion process, we generate the LJSpeech set and measure likelihood at 8 equally-spaced intervals of  $t$ , we expect that likelihood increases as  $t$  decreases. We measure likelihood in Bits-Per-Dimension (BPD),  $-\log p(\mathbf{X}) \log_2 \exp \cdot (\Pi_i \mathbf{d}_i)^{-1}$ , where  $d$  is the shape of  $\mathbf{X}$ . Lower BPD means higher likelihood. Table 1 shows that although likelihood increases as  $\mathbf{X}_T$  is denoised into data  $\mathbf{X}_0$ , the effect on other metrics is surprising. Mel-Cepstral Distortion (MCD) is a measure of how different two Mel-cepstra (audio

Table 1: Quantitative assessment of Grad-TTS from time 1 to 0.

| Metric  | Ref   | Time |      |      |      |      |      |      |      |       |
|---------|-------|------|------|------|------|------|------|------|------|-------|
|         |       | 1.00 | 0.88 | 0.75 | 0.62 | 0.50 | 0.38 | 0.25 | 0.12 | 0.00  |
| BPD ↓   | -0.06 | 2.79 | 2.79 | 2.79 | 2.79 | 2.77 | 2.72 | 2.55 | 1.35 | -0.08 |
| LogF0 ↓ | 0.00  | 0.28 | 0.28 | 0.28 | 0.28 | 0.28 | 0.27 | 0.27 | 0.27 | 0.27  |
| MCD ↓   | 0.00  | 6.52 | 6.52 | 6.52 | 6.50 | 6.47 | 6.43 | 6.39 | 6.34 | 6.31  |
| WER ↓   | 0.03  | 0.08 | 0.08 | 0.08 | 0.09 | 0.08 | 0.10 | 0.13 | 0.16 | 0.19  |
| ASV ↑   | 1.00  | 0.74 | 0.74 | 0.73 | 0.73 | 0.74 | 0.75 | 0.78 | 0.84 | 0.86  |

features) are from each other (Kominek et al., 2008).<sup>3</sup> We note the root mean squared error of the log fundamental frequencies as “LogF0”, this measures pitch/intonation accuracy.<sup>4</sup> Word Error Rate (WER) is the ratio of transcription errors to the number of words; to measure intelligibility we calculate the WER of the transcript generated by the Automatic Speech Recognition (ASR) foundation model Whisper (Radford et al., 2022). We measure speaker similarity (ASV) by comparing the cosine similarity between embeddings from the speaker verification foundation model Titanet (Koluguri et al., 2021). Likelihood is correlated to ASV, marginally with MCD, but not LogF0. WER increases as likelihood improves. The results suggest that composition between the source text and hypothesis utterance<sup>5</sup> is modelled by the encoder  $\mathbf{E}_\theta(\cdot)$ , and the diffusion decoder does not model the exact likelihood between text and speech  $p_0(\mathbf{X}|\mathbf{y})$ . We verify this through an ASR decoder rescoring experiment on LJSpeech. An ASR pipeline generates a list of hypothesis transcripts for a given utterance, which are scored by a weighted combination of an Acoustic model (AM) score and a language model score to find the best transcription. We view this pipeline as a diagnostic tool for how well Grad-TTS likelihoods can measure speech/text compatibility. We replace the AM score with Grad-TTS likelihoods and execute standard hypothesis rescoring techniques (Kahn et al., 2022). We test a wav2vec2 model finetuned on 10 minutes of audiobook data (Panayotov et al., 2015), and Whisper (Table 2). In all cases, the DM

3. We calculate MCD with the method presented in ESPnet (Gao et al., 2023)

4. For reference, Tacotron 2 and Fastspeech 2 achieve 0.26 and 0.24 LogF0 respectively (Ren et al., 2022).

5. The ASR output

Table 2: WER%  $\downarrow$  of n-best list rescoring strategies including Grad-TTS.

| AM Model | AM Score | Grad-TTS LL | Oracle Best | Oracle worst | Random |
|----------|----------|-------------|-------------|--------------|--------|
| wav2vec2 | 13.3     | 19.6        | 10.5        | 29.0         | 20.2   |
| Whisper  | 3.3      | 4.7         | 1.5         | 7.2          | 4.3    |

likelihoods yield a worse score than the AM, although better than the oracle worst for both AMs.<sup>6</sup> This suggests that the likelihoods may have some sensitivity to textual changes but lack an expressive linguistic representation. To survey how DM likelihood interacts with intelligibility and speaker quality, we employ Grad-TTS to adapt TED-LIUM live-talk data (Rousseau et al., 2012) to aid an ASR model trained on audiobooks. ASR models perform worse when the acoustic properties differ between train and test data. We pass the spectrogram through a Gaussian blur with kernel 5 and  $\sigma = 1$ , simulating text encoder output  $\mathcal{N}(\mathbf{X}) \approx \mathbf{E}_\theta(\mathbf{y})$ .<sup>7</sup> The forward ODE is used to calculate  $\mathbf{X}_T$ ,  $\mathbf{X}_0$  is produced with the reverse ODE thereafter. Given that Grad-TTS is trained on LJSpeech, the newly generated  $\mathbf{X}_0$  will be acoustically similar to the data the ASR model was trained on. WER will be reduced if Grad-TTS can successfully adapt between live-talk and audiobook domains. We experiment with both Euler and RK45 solvers (Table 3). The Euler method produces

Table 3: Quantitative assessment of cross-domain adaptation with Grad-TTS.

| ODE sampler |         | Metric           |                  |                |
|-------------|---------|------------------|------------------|----------------|
| Forward     | Reverse | WER $\downarrow$ | BPD $\downarrow$ | ASV $\uparrow$ |
| None        | None    | 0.46             | 1.66             | 0.52           |
| Euler       | Euler   | 0.94             | -1.47            | 0.66           |
| RK45        | Euler   | 0.57             | 6.92             | 0.54           |
| RK45        | RK45    | 0.57             | 1.83             | 0.55           |

unintelligible audio, yet has high speaker similarity and improved likelihood (BPD). The RK45 sampler degrades intelligibility to a lesser degree than Euler, but speaker adaptation is negligible. The trend is that greater shift towards the LJSpeech speaker (ASV increases) produces less intelligible audio (WER increases).

## 4.2. Text-to-image

Datasets considered are PACS (Li et al., 2017), a domain generalisation dataset that includes images of 9 classes in 4 domains (photo, art, cartoon, sketch) and CLEVR (Johnson et al., 2017), a diagnostic dataset containing synthetic images of 3 3D objects of 8 colours. We use images generated from Lewis et al. (2023) e.g. a “red sphere” (Figure 1(a)). We use a subset of CLEVR consisting of single objects. For both datasets we repeat each

6. Although Grad-TTS performs better than random for the wav2vec2 hypothesis list, this result is insignificant for an 82% confidence interval with the matched-pairs significance test (Gillick and Cox, 1989).

7. This method is further explained in Appendix A

class-domain/shape-colour pair 20 times. Images are resized to  $512^2/1024^2$ . We report the likelihood of SDXL, where we use CFG to generate PACS. We compute FID and CLIP similarity to measure image quality and compatibility respectively (Table 4.2). FID measures

Table 4: The SDXL generative process from  $t = 1$  to 0 with CFG=7 at 1024 resolution.

| Metric | Data  | Time   |        |        |        |        |
|--------|-------|--------|--------|--------|--------|--------|
|        |       | 1.00   | 0.75   | 0.50   | 0.25   | 0.00   |
| BPD ↓  | -0.17 | 0.07   | 0.08   | -0.08  | -0.12  | -0.08  |
| FID ↓  | 0.00  | 478.91 | 369.91 | 225.89 | 221.40 | 229.08 |
| CLIP ↑ | 29.50 | 22.72  | 23.49  | 28.10  | 27.97  | 28.16  |

the distance between real and synthetic image distributions. CLIP measures the compatibility between prompts and images. These metrics can be related to MCD and WER in the TTS experiment. Similar to Table 1, FID and BPD both decrease, suggesting that the generative process improves sample quality and likelihood with respect to  $t$ . Although there is a clear trend that FID does decrease over time, it is higher than typical.<sup>8</sup> It is assumed that this is because SDXL was trained on more data than PACS, thus generating many samples absent in the PACS dataset. Unlike Grad-TTS, the conditional metric (CLIP) improves, showing that CFG expresses a more conditional likelihood than the MR-VP SDE that used by Grad-TTS. Table 5 shows setting a higher CFG scale intuitively produces

Table 5: Impacts of CFG, reconstruction (-R) and image sizes.

| Metric | Data  | CFG    |        |        |        | Size-Reconstruct |        |        |        |
|--------|-------|--------|--------|--------|--------|------------------|--------|--------|--------|
|        |       | 0.00   | 3.00   | 5.00   | 7.00   | 512              | 512-R  | 1024   | 1024-R |
| BPD ↓  | -0.17 | -0.04  | -0.05  | -0.07  | -0.08  | 0.02             | -0.01  | 0.07   | -0.01  |
| FID ↓  | 0.00  | 300.98 | 249.67 | 227.14 | 229.08 | 406.39           | 406.26 | 478.91 | 480.34 |
| CLIP ↑ | 29.50 | 23.16  | 26.70  | 27.68  | 28.16  | 22.73            | 22.75  | 22.72  | 22.71  |

higher-likelihood samples. To measure how the generative process is intertwined with likelihood, we apply the forward process then backward process to an image producing an image similar to the original but with features more consistent to synthetic images. We dub this operation *reconstruction*.<sup>9</sup> Reconstruction increases likelihood without affecting other metrics, revealing inconsistency (Table 5). Lastly, we investigated visual-language reasoning, an important ability for TTI models. We are interested in observing whether DM likelihood can correctly match images to captions from a list of compositionally confounding captions. Although diffusion classifiers show that this is possible with proxy-likelihoods, can the same be said with exact likelihood? We evaluate the ability to discern objects on CLEVR. For each image, we present all confounding prompts e.g. the correct prompt is “a photo of a red sphere” but instead “a photo of a red cube” is provided. Accuracy is calculated based on the number of correct captions that were given the highest likelihood. We confound both colour and shape, but not at the same time. Correspondingly, we are

8. The DM in Song et al. (2021b) yields 2.92 FID on CIFAR-10.

9. An example is given in Appendix C



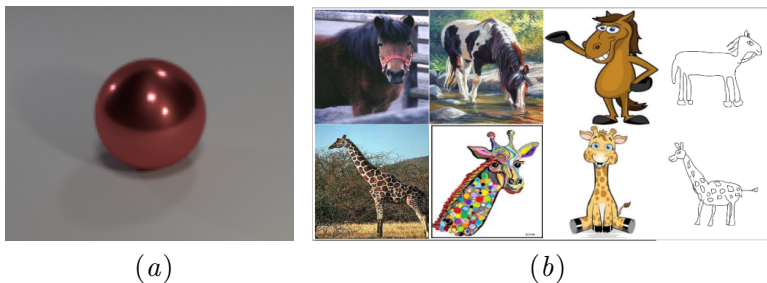


Figure 1: Example data from CLEVR (a) and PACS (b)

interested in other visual-language concepts. Complementary to the CLEVR experiment, we use PACS to measure the likelihood sensitivity to object vs domain changes e.g. a photo of a horse (Figure 1(b)). The results are shown in Table 6. It can be seen that the scores

Table 6: Prompt accuracy on CLEVR and PACS

| Params       |     | CLEVR  |       | PACS  |        |
|--------------|-----|--------|-------|-------|--------|
| Reconstruct  | CFG | Colour | Shape | Class | Domain |
| $\times$     | 0   | 12     | 33    | 86    | 50     |
|              | 3   | 0      | 33    | 0     | 0      |
|              | 5   | 25     | 33    | 0     | 0      |
| $\checkmark$ | 0   | 38     | 33    | 14    | 0      |
|              | 3   | 12     | 0     | 14    | 0      |
|              | 5   | 12     | 0     | 0     | 0      |
| Random       |     | 12     | 33    | 11    | 25     |
| CLIP-score   |     | 63     | 67    | 100   | 100    |

are unexpectedly low. We also provide scores from random selection and when selecting captions with the highest CLIP score. The results on CLEVR are comparable to random choice, when reconstruction is used, shape accuracy is reduced. SDXL performs better on PACS without reconstruction and guidance. This is anomalous behaviour since the rest of the PACS results are typically 0% accuracy.

## 5. Conclusion

Given that DMs are trained to maximise the VLB of likelihood, it is important to understand the nuances of this exact likelihood. This is especially true for conditional tasks where the conditional likelihood is often modelled implicitly, such as with a MR-VP SDE, or with CFG. We show that any reasonable assumptions should be verified as the task and conditional ODE used has substantial impact on the nature of DM likelihood. For Grad-TTS, the MR-VP SDE likelihood models speaker characteristics and smooth spectrograms, but not features of language. Such findings are contrary to what one would expect for a



probabilistic conditional process between speech and text. For SDXL, CFG does appear to model prompt-faithful image generation, but exact likelihood from SDXL cannot be used for prompt classification. This is inconsistent with the concept of Diffusion Classifiers that use lower bounds on likelihood for classification. Hence, we quantitatively show a current lack of understanding of DM likelihood. This paper represents introductory evidence that more attention should be placed in experiments and theoretical understanding in DM likelihood, especially on conditional tasks.

## Limitations

This paper intends to demonstrate the potential adverse effects of introducing (implicit) conditioning mechanisms into frameworks originally studied for unconditional modelling. This paper does not provide any theoretical explanations to the unexpected behaviour observed, nor are any new explicit conditional likelihood methods derived. This paper has only explored two types of conditional generation, and only with their respective “iconic” model, whether this generalises to all diffusion models is unknown. Diffusion models are an instance of a continuous normalizing flow, a natural extension is to observe if other continuous normalizing flows e.g. flow-matching models exhibit the same behaviour.

## Acknowledgments

We thank Peter Vickers for his helpful knowledge of the CLIP model, Kane O’Reagan & Shaun Cassini for proof-reading, and Xiaozhou Tan for help with figures. This work was supported by the Centre for Doctoral Training in Speech and Language Technologies (SLT) and their Applications funded by UK Research and Innovation [grant number EP/S023062/1].

## References

- Brian D. O. Anderson. Reverse-time diffusion equation models. *Stochastic Processes and their Applications*, 12(3):313–326, May 1982. ISSN 0304-4149. doi: 10.1016/0304-4149(82)90051-5.
- Ricky T. Q. Chen, Yulia Rubanova, Jesse Bettencourt, and David Duvenaud. Neural Ordinary Differential Equations, December 2019.
- Kevin Clark and Priyank Jaini. Text-to-Image Diffusion Models are Zero-Shot Classifiers, September 2023.
- J. R. Dormand and P. J. Prince. A family of embedded Runge-Kutta formulae. *Journal of Computational and Applied Mathematics*, 6(1):19–26, March 1980. ISSN 0377-0427. doi: 10.1016/0771-050X(80)90013-3.
- Dongji Gao, Jiatong Shi, Shun-Po Chuang, Leibny Paola Garcia, Hung-yi Lee, Shinji Watanabe, and Sanjeev Khudanpur. EURO: ESPnet Unsupervised ASR Open-source Toolkit, May 2023.

- L. Gillick and S.J. Cox. Some statistical issues in the comparison of speech recognition algorithms. *International Conference on Acoustics, Speech, and Signal Processing*, pages 532–535, 1989. doi: 10.1109/ICASSP.1989.266481.
- Mark S. Graham, Walter H. L. Pinaya, Petru-Daniel Tudosiu, Parashkev Nachev, Sebastien Ourselin, and Jorge Cardoso. Denoising Diffusion Models for Out-of-Distribution Detection. In *Proceedings of the IEEE/CVF Conference on Computer Vision and Pattern Recognition*, pages 2947–2956, 2023.
- Will Grathwohl, Ricky T. Q. Chen, Jesse Bettencourt, Ilya Sutskever, and David Duvenaud. FFDJORD: Free-form Continuous Dynamics for Scalable Reversible Generative Models, October 2018.
- Jonathan Ho and Tim Salimans. Classifier-Free Diffusion Guidance, July 2022.
- Jonathan Ho, Ajay Jain, and Pieter Abbeel. Denoising Diffusion Probabilistic Models. In *Advances in Neural Information Processing Systems*, volume 33, pages 6840–6851. Curran Associates, Inc., 2020.
- Hailong Hu and Jun Pang. Membership Inference of Diffusion Models, January 2023.
- Michael F Hutchinson. A stochastic estimator of the trace of the influence matrix for Laplacian smoothing splines. *Communications in Statistics-Simulation and Computation*, 18(3):1059–1076, 1989. ISSN 0361-0918.
- Aapo Hyvärinen. Estimation of Non-Normalized Statistical Models by Score Matching. *Journal of Machine Learning Research*, 6(24):695–709, 2005. ISSN 1533-7928.
- Gabriel Gabriel Ilharco, Wortsman, Mitchell and, Carlini, Nicholas and, Taori, Rohan and, Dave, Achal and, Shankar, Vaishaal and, Namkoong, Hongseok and, Miller, John and, Hajishirzi, Hannaneh and, Farhadi, Ali and, and Schmidt, Ludwig. OpenCLIP. *Zenodo*, June 2021. doi: 10.5281/zenodo.5143773.
- Keith Ito and Linda Johnson. The LJ Speech Dataset. <https://keithito.com/LJ-Speech-Dataset>, 2017.
- Justin Johnson, Bharath Hariharan, Laurens van der Maaten, Li Fei-Fei, C. Lawrence Zitnick, and Ross Girshick. CLEVR: A Diagnostic Dataset for Compositional Language and Elementary Visual Reasoning. In *Proceedings of the IEEE Conference on Computer Vision and Pattern Recognition*, pages 2901–2910, 2017.
- Jacob D. Kahn, Vineel Pratap, Tatiana Likhomanenko, Qiantong Xu, Awni Hannun, Jeff Cai, Paden Tomasello, Ann Lee, Edouard Grave, Gilad Avidov, Benoit Steiner, Vitaliy Liptchinsky, Gabriel Synnaeve, and Ronan Collobert. Flashlight: Enabling Innovation in Tools for Machine Learning. In *Proceedings of the 39th International Conference on Machine Learning*, pages 10557–10574. PMLR, June 2022.
- Nithin Rao Koluguri, Taejin Park, and Boris Ginsburg. TitaNet: Neural Model for speaker representation with 1D Depth-wise separable convolutions and global context, October 2021.

- John Kominek, Tanja Schultz, and Alan W Black. Synthesizer voice quality of new languages calibrated with mean mel cepstral distortion. In *SLTU*, pages 63–68, 2008.
- Martha Lewis, Nihal V. Nayak, Peilin Yu, Qinan Yu, Jack Merullo, Stephen H. Bach, and Ellie Pavlick. Does CLIP Bind Concepts? Probing Compositionality in Large Image Models, March 2023.
- Alexander C. Li, Mihir Prabhudesai, Shivam Duggal, Ellis Brown, and Deepak Pathak. Your Diffusion Model is Secretly a Zero-Shot Classifier, September 2023.
- Da Li, Yongxin Yang, Yi-Zhe Song, and Timothy M. Hospedales. Deeper, Broader and Artier Domain Generalization. In *Proceedings of the IEEE International Conference on Computer Vision*, pages 5542–5550, 2017.
- Cheng Lu, Kaiwen Zheng, Fan Bao, Jianfei Chen, Chongxuan Li, and Jun Zhu. Maximum Likelihood Training for Score-Based Diffusion ODEs by High-Order Denoising Score Matching, June 2022.
- Vassil Panayotov, Guoguo Chen, Daniel Povey, and Sanjeev Khudanpur. Librispeech: An ASR corpus based on public domain audio books. In *2015 IEEE International Conference on Acoustics, Speech and Signal Processing (ICASSP)*, pages 5206–5210, April 2015. doi: 10.1109/ICASSP.2015.7178964.
- Dustin Podell, Zion English, Kyle Lacey, Andreas Blattmann, Tim Dockhorn, Jonas Müller, Joe Penna, and Robin Rombach. SDXL: Improving Latent Diffusion Models for High-Resolution Image Synthesis, July 2023.
- Vadim Popov, Ivan Vovk, Vladimir Gogoryan, Tasnima Sadekova, and Mikhail Kudinov. Grad-TTS: A Diffusion Probabilistic Model for Text-to-Speech, August 2021.
- Vadim Popov, Ivan Vovk, Vladimir Gogoryan, Tasnima Sadekova, Mikhail Kudinov, and Jiansheng Wei. Diffusion-Based Voice Conversion with Fast Maximum Likelihood Sampling Scheme, August 2022.
- Alec Radford, Jong Wook Kim, Chris Hallacy, Aditya Ramesh, Gabriel Goh, Sandhini Agarwal, Girish Sastry, Amanda Askell, Pamela Mishkin, Jack Clark, Gretchen Krueger, and Ilya Sutskever. Learning Transferable Visual Models From Natural Language Supervision, February 2021.
- Alec Radford, Jong Wook Kim, Tao Xu, Greg Brockman, Christine McLeavey, and Ilya Sutskever. Robust Speech Recognition via Large-Scale Weak Supervision, December 2022.
- Yi Ren, Chenxu Hu, Xu Tan, Tao Qin, Sheng Zhao, Zhou Zhao, and Tie-Yan Liu. Fast-Speech 2: Fast and High-Quality End-to-End Text to Speech, August 2022.
- Olaf Ronneberger, Philipp Fischer, and Thomas Brox. U-Net: Convolutional Networks for Biomedical Image Segmentation, May 2015.

- Anthony Rousseau, Paul Deléglise, and Yannick Estève. TED-LIUM: An Automatic Speech Recognition dedicated corpus. In *Proceedings of the Eighth International Conference on Language Resources and Evaluation (LREC'12)*, pages 125–129, Istanbul, Turkey, May 2012. European Language Resources Association (ELRA).
- John Skilling. The eigenvalues of mega-dimensional matrices. *Maximum Entropy and Bayesian Methods: Cambridge, England, 1988*, pages 455–466, 1989. ISSN 9048140447.
- Jascha Sohl-Dickstein, Eric Weiss, Niru Maheswaranathan, and Surya Ganguli. Deep Un-supervised Learning using Nonequilibrium Thermodynamics. In *Proceedings of the 32nd International Conference on Machine Learning*, pages 2256–2265. PMLR, June 2015.
- Jiaming Song, Chenlin Meng, and Stefano Ermon. Denoising Diffusion Implicit Models, October 2022.
- Yang Song, Sahaj Garg, Jiaxin Shi, and Stefano Ermon. Sliced Score Matching: A Scalable Approach to Density and Score Estimation, June 2019.
- Yang Song, Conor Durkan, Iain Murray, and Stefano Ermon. Maximum Likelihood Training of Score-Based Diffusion Models, October 2021a.
- Yang Song, Jascha Sohl-Dickstein, Diederik P. Kingma, Abhishek Kumar, Stefano Ermon, and Ben Poole. Score-Based Generative Modeling through Stochastic Differential Equations. In *International Conference on Learning Representations*, February 2021b.
- Lucas Theis, Aäron van den Oord, and Matthias Bethge. A note on the evaluation of generative models, April 2016.
- Pascal Vincent. A Connection Between Score Matching and Denoising Autoencoders. *Neural Computation*, 23(7):1661–1674, July 2011. ISSN 0899-7667. doi: 10.1162/NECO\_a\_00142.
- Ling Yang, Zhilong Zhang, Yang Song, Shenda Hong, Runsheng Xu, Yue Zhao, Wentao Zhang, Bin Cui, and Ming-Hsuan Yang. Diffusion Models: A Comprehensive Survey of Methods and Applications, March 2023.

## Appendix A. Grad-TTS encoder and decoder output

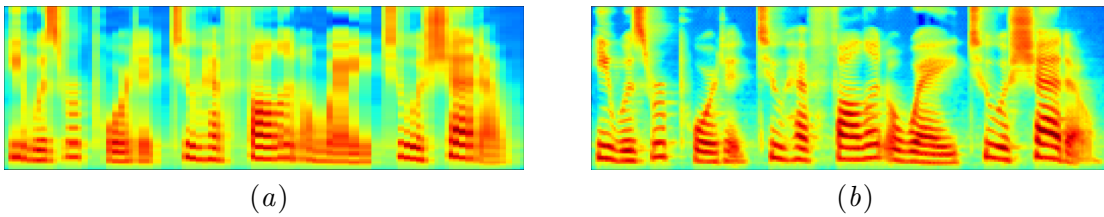


Figure 2: Grad-TTS encoder output (a) and decoder output (b). The encoder produces intelligible spectrograms, and the decoder removes distortion and encourages speaker characteristics. The fact that the encoder output is similar to distorted spectrograms is core to the unsupervised domain adaptation method in Table 3 where blurry spectrograms are treated as input to the diffusion decoder.

## Appendix B. Additional tables

Table 7: Various metrics during the generative process over time. The image distribution quality (FID) and prompt accuracy (CLIP) improve, as does the likelihood (BPD). The best results are found at 1024 resolution with a high guidance scale.

| CFG | pipe height | r | BPD   | 1.00 FID | CLIP  | BPD   | 0.75 FID | CLIP  | BPD   | 0.50 FID | CLIP  | BPD   | 0.25 FID | CLIP  | BPD   | 0.00 FID | CLIP  |
|-----|-------------|---|-------|----------|-------|-------|----------|-------|-------|----------|-------|-------|----------|-------|-------|----------|-------|
| 0   | 512         | ✗ | 0.02  | 417.58   | 22.58 | 0.02  | 399.30   | 23.62 | -0.01 | 310.19   | 22.68 | -0.01 | 308.96   | 22.23 | -0.01 | 310.24   | 22.55 |
| 3   | 512         |   | 0.02  | 412.40   | 22.60 | 0.02  | 391.65   | 23.90 | -0.01 | 280.20   | 23.75 | -0.02 | 279.52   | 23.45 | -0.01 | 278.99   | 23.66 |
| 5   | 512         |   | 0.02  | 409.33   | 22.67 | 0.02  | 378.74   | 24.18 | -0.02 | 268.82   | 24.36 | -0.02 | 268.72   | 23.95 | -0.02 | 264.01   | 24.35 |
| 7   | 512         |   | 0.02  | 406.39   | 22.73 | 0.02  | 373.26   | 24.31 | -0.02 | 257.55   | 24.63 | -0.03 | 257.93   | 24.31 | -0.02 | 257.00   | 24.56 |
| 0   | 512         | ✓ | 0.01  | 417.80   | 22.58 | 0.00  | 399.60   | 23.61 | -0.01 | 309.89   | 22.65 | -0.02 | 308.74   | 22.23 | -0.01 | 311.61   | 22.57 |
| 3   | 512         |   | -0.00 | 412.18   | 22.60 | -0.00 | 392.58   | 23.93 | -0.02 | 282.78   | 23.87 | -0.02 | 278.91   | 23.47 | -0.02 | 280.99   | 23.67 |
| 5   | 512         |   | -0.01 | 408.25   | 22.68 | -0.01 | 374.78   | 24.19 | -0.02 | 269.79   | 24.41 | -0.03 | 266.02   | 24.08 | -0.02 | 265.90   | 24.28 |
| 7   | 512         |   | -0.01 | 406.26   | 22.75 | -0.01 | 373.70   | 24.31 | -0.02 | 256.47   | 24.63 | -0.03 | 256.94   | 24.36 | -0.02 | 259.19   | 24.66 |
| 0   | 1024        | ✗ | 0.07  | 478.22   | 22.59 | 0.08  | 418.89   | 21.98 | -0.04 | 300.59   | 23.00 | -0.06 | 309.11   | 22.99 | -0.04 | 300.98   | 23.16 |
| 3   | 1024        |   | 0.07  | 478.30   | 22.65 | 0.08  | 399.29   | 22.51 | -0.05 | 245.04   | 26.55 | -0.08 | 251.32   | 26.59 | -0.05 | 249.67   | 26.70 |
| 5   | 1024        |   | 0.07  | 478.65   | 22.70 | 0.08  | 380.89   | 23.04 | -0.07 | 231.44   | 27.72 | -0.10 | 232.38   | 27.69 | -0.07 | 227.14   | 27.68 |
| 7   | 1024        |   | 0.07  | 478.91   | 22.72 | 0.08  | 369.91   | 23.49 | -0.08 | 225.89   | 28.10 | -0.12 | 221.40   | 27.97 | -0.08 | 229.08   | 28.16 |
| 0   | 1024        | ✓ | 0.06  | 478.22   | 22.59 | 0.08  | 418.82   | 21.97 | -0.04 | 300.53   | 23.02 | -0.06 | 308.12   | 22.99 | -0.04 | 301.76   | 23.17 |
| 3   | 1024        |   | 0.05  | 479.91   | 22.65 | 0.03  | 402.99   | 22.49 | -0.06 | 252.33   | 26.55 | -0.09 | 263.05   | 26.60 | -0.06 | 255.12   | 26.77 |
| 5   | 1024        |   | 0.02  | 480.88   | 22.68 | 0.00  | 384.40   | 23.01 | -0.07 | 239.35   | 27.69 | -0.11 | 241.89   | 27.66 | -0.07 | 235.62   | 27.73 |
| 7   | 1024        |   | -0.01 | 480.34   | 22.71 | -0.01 | 375.69   | 23.43 | -0.09 | 231.81   | 27.96 | -0.13 | 228.23   | 27.95 | -0.09 | 234.73   | 28.10 |

## Appendix C. SDXL Images



(a)



(b)

Figure 3: A source image (a) and a reconstructed image (b), with caption “panda eating cake”. The panda and orientation are preserved but the domain has changed. The cake has been absorbed.